Microstructure, flow behavior, and bulk texture evolution of cold drawn copper-silver composites

S. Dodla[a,*], P. Thiem[b], M. Krüger[b], D. Dietrich[c], A. Bertram[a]

[a] *Institut für Mechanik, Otto-von-Guericke-Universität Magdeburg, D-39106, Magdeburg Germany*
[b] *Institut für Werkstoff- und Fügetechnik, Otto-von-Guericke-Universität Magdeburg, D-39106, Magdeburg Germany*
[c] *Institut für Werkstoffwissenschaft und Werkstofftechnik, Technische Universität Chemnitz, D-09107, Chemnitz, Germany*

Abstract

In the last 20 years, several groups used nanostructured composites to produce high strength conductor materials for magnetic applications. The mechanical strength of Cu-Ag composites is strongly influenced by metal forming operations. Within the scope of the paper, the microstructure, the mechanical behavior, and the texture evolution are investigated for two cold drawn Cu-63wt%Ag composite rods. The aim of these investigations is to understand the influence of the microstructure and texture evolution on the mechanical behavior. The investigation is carried out using optical microscopy, scanning electron microscopy (SEM) along with electron backscattered diffraction (EBSD), X-ray diffraction measurements (XRD), and compression testing. The microscopic images show that the drawn samples mainly have a lamellar structure of Cu and Ag phases. However, elliptical shaped regions of primarily solidified copper solid solution are also observed. With increase of plastic deformation, the average lamella thickness of both phases has been decreased. EBSD measurements show that abundant banded regions are observed in the Ag phase while very few banded regions are present in the Cu phase. The bulk XRD measurements reveal that both phases of the drawn samples initially have the same type of texture, and both phases develop the same brass-type $[110]\langle 112\rangle$ texture. The texture intensity increases for both phases as the drawing strain increases. Compression tests are performed at constant strain rate of $10^{-4}s^{-1}$ at room temperature. The stress-strain curves under compression are presented for two different drawn samples. The texture measurements after compression reveal that the texture becomes more pronounced.

Keywords: Cu-Ag composite, cold drawn, lamellar phase structure, electron backscattered diffraction (EBSD), X-ray diffraction (XRD), compression testing, texture measurement

1. Introduction

Copper based composites (Cu-Ag, Cu-Be, Cu-Nb, etc.) are used as high-strength conductors in pulse magnets, hybrid magnets, and resistive (bitter) magnets because of their unique combination of high mechanical strength and high electrical conductivity [1, 2, 3, 4]. In general, two-phase Cu-Ag composites containing 6-72 wt% Ag are used as conductor materials for the application in magnets produced by cold drawing along with intermediate heat treatments [5, 6, 7, 8, 9]. The microstructure will strongly influence the mechanical properties of Cu-Ag composites [10]. By changing the concentration of Ag in Cu-based composites and also different processing methods, the morphology and texture result in anisotropy of the mechanical properties. Therefore, various new and improved Cu-Ag composites have been used in the field of magnetic applications. However, some questions have to be answered, such as: (1) what is the appropriate Cu-Ag composition,

*Corresponding author. Tel. +49 391 67 52246; Fax +49 391 67 2863
Email address: srihari.dodla@st.ovgu.de (S. Dodla)

and (2) what processing technique develops the required mechanical properties. For example, with increase in the concentration of Ag, i.e., 7 wt%, 24 wt%, 72 wt%, the ultimate tensile strength increases with increase in the drawing strain [11]. Furthermore, the strength level can be increased by an appropriate heat treatment [12, 11]. In the study by Heringhaus [13], compression and tensile tests have been conducted for Cu-72 wt%Ag eutectic composites, in which the mechanical properties are presented as a function of the wire deformation. Following cold-drawing to high strains, the eutectic Cu-Ag composites develop an ultimate tensile strength as high as 1.15 GPa [13]. During the metal forming operation by cold working, the lamellar nature of these two phases, one a Cu-rich, and the other an Ag-rich solid solution, have been compressed and elongated resulting in a fine and dense structure. The phase boundaries and grain boundaries of these two phases block the dislocation movement through the alloy, causing an increase in strength of the material. Therefore, such work-hardened composites containing a fine layer structure, show higher strength than that expected from a simple rule of mixture [14, 5, 15]. Following cold drawing operations, the Cu-Ag composite experiences microstructural changes. Therefore, the rods produced by drawing exhibit anisotropic properties. An important example of an anisotropy is the crystallographic texture.
Many studies of the texture evolution during large plastic deformations have been concentrated on single phase metals. For example, the texture evolution of silver has been examined during equal channel angular extrusion (ECAE) [16, 17]. In the case of two phase Cu-based composites, the presence of the second phase will affect the texture evolution. In the recent work, these effects have been studied for Cu-Nb composites under plastic deformation by accumulative roll bonding [18, 19]. Recently, the local and global texture analysis of CuAl alloys have been examined by wire drawing, where microstructure change has been investigated by varying the stacking fault energy [20]. The texture evolution of an eutectic Cu-Ag composite for different rolling reductions has been described by [21]. As they report, the alloy-type rolling texture is found for both Cu and Ag phases. An unusual texture in the Cu phase of the Cu-Ag eutectic composite has been observed, and explained in terms of twinning mechanism, i.e., Ag contributes propagation of twins into Cu. Of these different methods, the most common and simple method for strengthening composites includes cold drawing (strain hardening) [22]. It is clear that the texture of different drawing reductions also influences the mechanical properties. Besides, the effect of texture in the near-eutectic cold drawn Cu-63 wt%Ag composite due to plastic deformation on the mechanical properties has not yet been reported. With increase in the cold drawing operation, the mechanical strength is increased, and the texture increases significantly. We performed the experimental investigations on two differently cold drawn Cu-Ag rods to estimate the texture evolution and also to study the influence of the mechanical behavior. These rods (diameters d_1, d_2) with drawing reductions $\eta_1 = 0.9$ and $\eta_2 = 2.1$ ($\eta = ln(A_0/A)$), respectively, are chosen to determine the benefits and limitations in producing high strength conductor materials, where A_0 and A are the initial and the current cross section of the specimen, respectively.

In the present work, near-eutectic (Cu-63wt%Ag) cold drawn samples of diameter 12.42 mm and 6.73 mm are examined to determine the influences that changes in the microstructure and texture, have on the mechanical behavior. The microstructural refinement and the anisotropy are accompanied by the evolution of texture. This understanding of the development of texture in the rods will provide a basis for the development of new conductor materials with optimum microstructure. Besides the detailed microstructural investigation of the cold-drawn Cu-Ag rods, this work also reports the significance of the anisotropy of two different rods to the development of the conductor materials. The investigation has been carried out using optical and scanning electron microscopy, electron backscattered diffraction (EBSD), X-ray diffraction (XRD), and compression testing. Macro-texture XRD measurements show that both Ag and Cu phases develop a brass-type texture, which is also present after compression tests with different intensities. The EBSD measurements reveal that the Ag phase consists of shear bands or twinned regions, while in the Cu-phase very few shear bands or twinned regions are observed. The brass-type $\{110\}\langle 112\rangle$ texture expected for the Ag-phase and not for the Cu-phase, has been discussed previously [21]. The metal or copper-type $\{112\}\langle 111\rangle$ texture is expected for rolled pure copper and its alloys

[23, 24]. Possibile reasons for this brass-type texture for the copper phase are presented in the section Results and discussion.

2. Experimental procedure

The Cu-Ag rods are supplied by the 'Allgemeine Gold- und Silberscheideanstalt' in Pforzheim, Germany. The material with initial diameter of 20 mm was processed by continuous casting. After casting, the rods are swaged to 20% reduction, and then cold drawn to reduction in diameter of 12.4 mm and 6.7 mm from a starting diameter at room temperature. Two different textured Cu-Ag rods (d_1, d_2) are examined to describe the microstructure development and the evolution of crystallographic texture. The samples are cut in both longitudinal and transverse directions for microstructural observations. The sample direction and the cutting plane are shown in Figure 1a. Figure 1b displays the cylindrical rods. In order to study the effect of the microstructure on the mechanical behavior, the samples are manufactured from the drawn rods in two different directions (longitudinal and transversal) by using an electric discharge machining (EDM) process. The samples are denoted by a symbol T in the transverse direction and L in the longitudinal direction. The samples are cold mounted in an epoxy resin, grinded using silica carbide (SiC) paper (180-2400 grit), machine polished with 3-μm diamond particles and a fine polish with 1-μm diamond particles using a water based lubricating solution. The specimens are chemically etched for 45 seconds in Nital solution (30% nitric acid in 70% ethanol) for imaging. After that a final OPS polishing step and an ion polishing with 3 kV Ar ions for one hour (GATAN PECS) was applied to obtain a smooth clean surface suitable for EBSD measurements. The samples are examined in a scanning electron microscope (FEI ESEM XL30 FEG equipped with EDX and EBSD) and in a reflected light microscope (Inverted light microscope ZEISS Axiovert 200 M equipped with Film and AxioCam MRc 5).

The uniaxial compression test is a simple test for the study of the flow behavior and also for

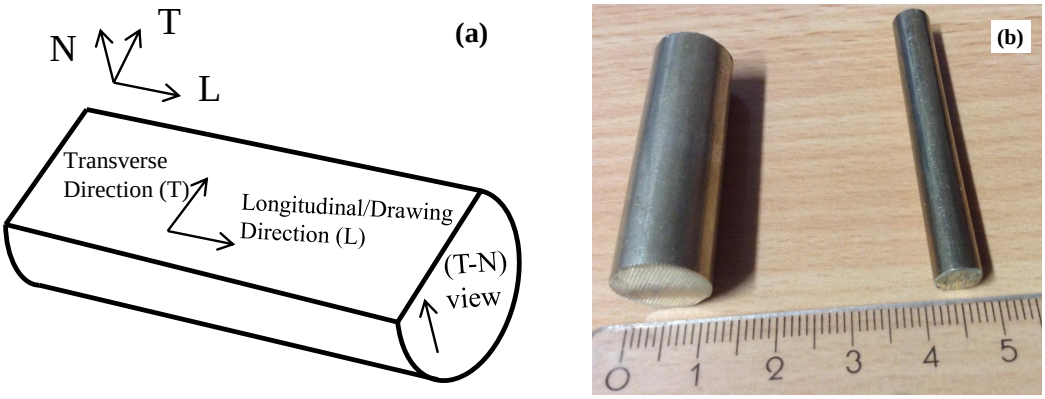

Figure 1: (a) schematic overview of a sample in different directions, (b) drawn sample of diameter $d_1 = 12.42$ mm and sample of diameter $d_2 = 6.73$ mm

the determination of the mechanical properties. In this type of test, the specimen shape allows more surface for texture measurements. The samples are tested in compression along longitudinal L and transversal T directions to gain a better understanding of the influence of different microstructure on the yield strength of the material. Besides the compression tests also shows the anisotropic nature of samples since the rods are cold drawn. The tests have been performed for both cylindrical samples in the two directions (longitudinal and transversal) on a universal testing machine (Zwick/Roell Z100). The tests are performed at a constant strain rate of $10^{-4}s^{-1}$ at room temperature. The initial dimensions of the specimen are 1.7 millimeters in diameter and

2.5 millimeters in height. To minimize the friction between the surface of the samples and the supporting holders, a Boron Nitride (BN) lubricant spray is used.

For the macro-texture using X-ray diffraction measurements (XRD), the samples (uncompressed, compressed) are mounted in a cold setting epoxy resin, are grinded using SiC sheets with grade numbers (P300, P480, P800, P1200, P2400, P4000) and machine polished with 3 μm diamond particles and finished using 1 μm. Finally, the samples are placed in the vibrating polishing machine for 20 hours using MasterMet 2 suspension. These samples are cleaned in ultrasonic cleaner for 10 min using isopropanol alcohol solution. For XRD measurements we used the X-ray diffractometer XRD3000PTS built by Rich. Seifert & Co. GmbH & Co. KG, Ahrensburg, Germany. The XRD3000PTS is a 4-axis diffractometer to analyze the phases and texture. We operated the measurements by using an X-ray tube with chromium anode in point focus mode and 1D-detector with secondary K_β filtering. Raw texture data is collected on metallographic samples using the texture measurement mode. Using the XRD software (Seifert Analyze Version 2.285), (111), (200) and (220) pole figures for copper solid solution crystals, and the (111), (200), (220), and (311) pole figures for silver solid solution crystals have been acquired. The MTEX software [25, 26, 27, 28] is used to reconstruct the orientation distribution function (ODF) from the XRD pole figures with the crystal orientation densities in a 3D orientation space defined by the three Euler angles ϕ_1, φ and ϕ_2. Textures in this article are presented in terms of (110), (111) pole figures and $\varphi_2\,(= 0°, 45°, 65°)$ sections of the ODF in the space of Euler angles $(\varphi_1, \phi) \leq 90$.

3. Results and discussion

3.1. Microstructure and initial texture of the sample d_1

Figure 2 presents the optical and SEM micrographs of the drawn sample d_1 in the transversal (T) and longitudinal (L) direction at different magnifications. Figure 2 A is an optical micrograph showing a grain structure with an average grain size of 50 μm. In Figure 2 B, C, the light phase is the Ag-rich phase and the dark phase is the Cu-rich phase. The microstructure is formed of a fine lamellar structure of Cu and Ag phases, and also elliptically shaped Cu inclusions (due to the drawing process) embedded in an Ag-rich matrix exist. The optical image in Figure 2 D shows an elongated grain structure in the longitudinal (L) direction, and the SEM micrograph in Figure 2 E, F shows a fine lamellar structure of Cu and Ag phases with an average lamella thickness of Cu (LT_{Cu}) of 65 nm and Ag (LT_{Ag}) of about 200 nm. The microstructural analysis shows that the grain boundaries at lower magnification and phase boundaries (lamellae interfaces) at higher magnification. The grain and phase boundaries of Cu and Ag will add obstacles to dislocation motion and hence influence the mechanical behavior of the composite.

It is clear that the anisotropy of metals is due to the crystallographic texture that is present in polycrystals. It has been shown that metal forming operations (drawing, rolling, extrusion) cause changes in the texture and, thus, also the influence the deformation response of the material [24, 18, 29]. We investigated the texture for the cold drawn sample d_1 by XRD measurements. For both phases (Ag, Cu) of the sample d_1, the XRD measured textures are plotted in Figure 3 and 4. Both Cu and Ag phases evolve the same alloy-type of texture. The texture components observed in the Ag and the Cu phase of the drawn sample are the stronger brass component ($\{110\}\langle 112\rangle$) and the weaker cube component ($\{001\}\langle 100\rangle$) with volume fractions that vary with orientations. It is clearly observed in the ODF plot that the φ_2 sections at 0° and 45° expose a strong brass component. Both phases have the same texture features with only small differences in the intensities, and are similar to those reported previously for the Cu-24wt%Ag rolled sheets [4]. The typical texture for the Cu phase is the copper type ($\{112\}\langle 111\rangle$) texture, while for the Ag phase it is the brass type ($\{110\}\langle 112\rangle$) texture [21]. From the results we see that the Ag phase has a strong brass component, and the deformation of the sample is mainly controlled by the Ag rich phase, and the lamellae orientation mainly along the brass system ($\{110\}\langle 112\rangle$). The texture is similar to the results obtained for rolled Ag by [30] and the eutectic Cu-72wt%Ag composite by [24].

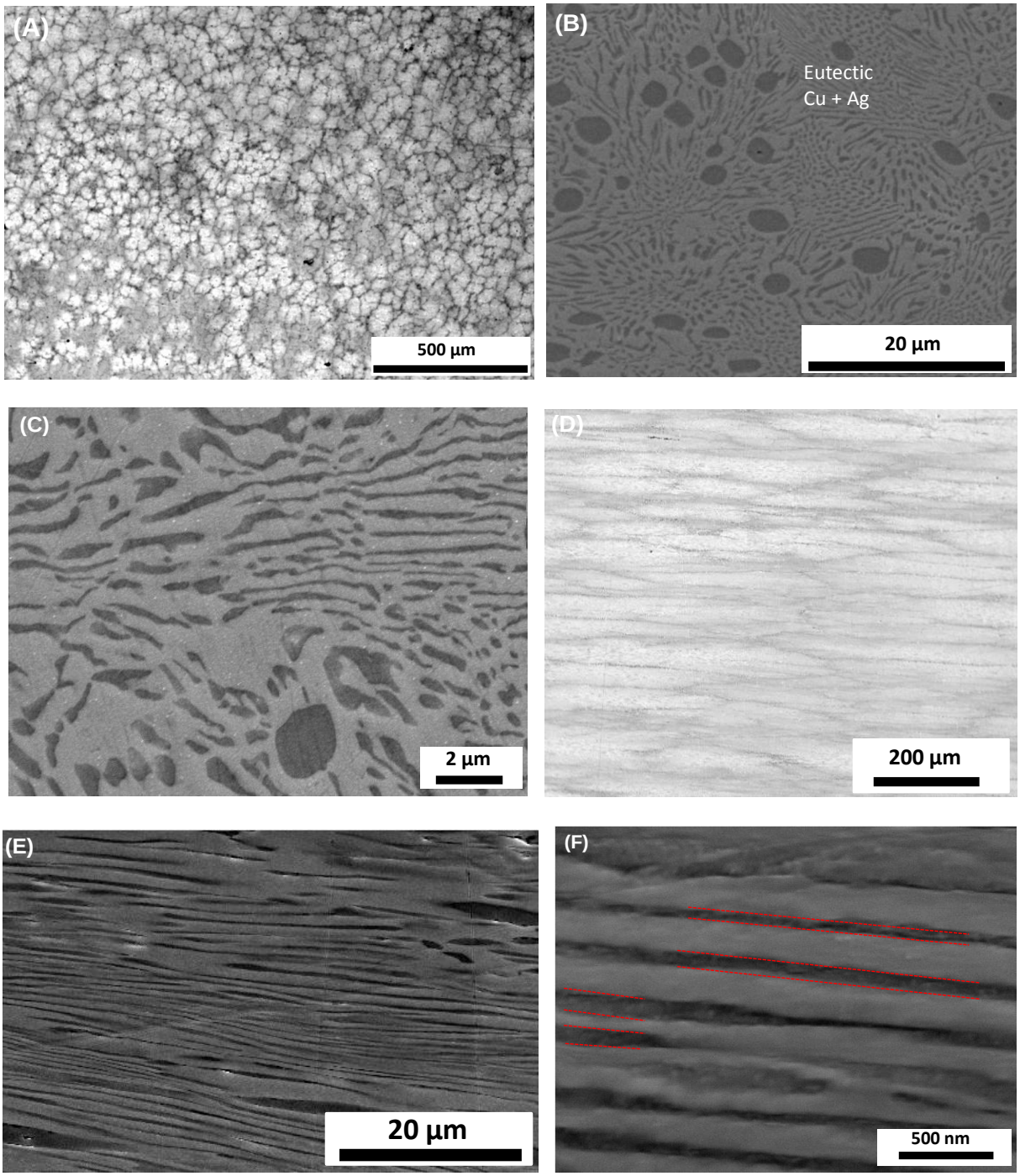

Figure 2: Microstructure of the Cu-Ag drawn sample (d_1): (A), (B), (C) transverse direction T, and (D), (E), (F) longitudinal direction L, analyzed by optical and scanning electron microscopy (SEM).

3.2. Microstructure and texture of drawn sample d_2

Figure 5 shows the microstructure of the sample d_2 in the transversal (T) and the longitudinal (L) directions. From the micrograph (see Figure 5 A), it has been observed that the grain size has been reduced from the center to the edge of the rod, since the outer surface experienced the highest deformation during the drawing operation. Also, the lamellae are curved because of the formation

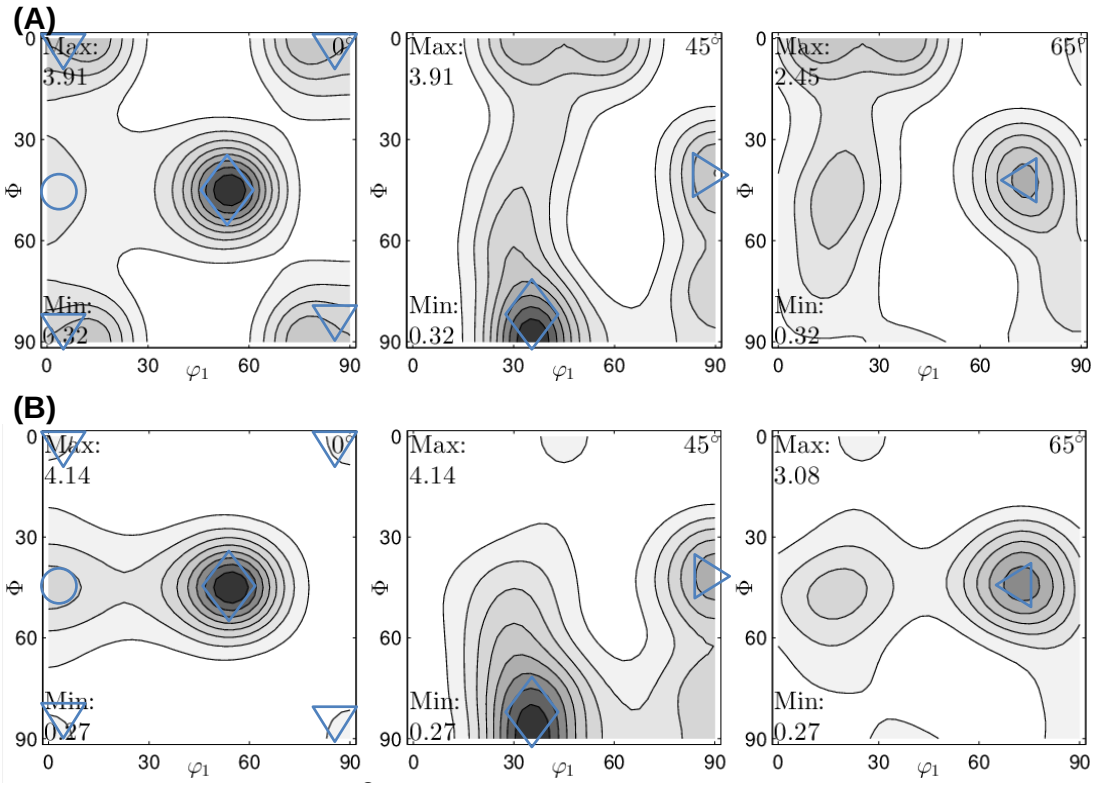

Figure 3: Sample d_1: ODF sections of $\varphi_2 = 0°, 45°, 65°$ in the space of Euler angles with locations of important texture components (∇ - cube orientation ($\{001\}\langle001\rangle$), $\diamondsuit$ - brass orientation ($\{110\}\langle112\rangle$), O - goss orientation ($\{011\}\langle100\rangle$), $\triangleright$ - copper orientation ($\{112\}\langle111\rangle$), $\triangleleft$ - S orientation ($\{123\}\langle634\rangle$)) (A) Ag phase, (B) Cu phase

of shear bands during the drawing process (see Figure 5 B). The final microstructure is due to the interaction of lamellae and shear bands. The micrograph (Figure 5 C, D) in the longitudinal direction reveals multilayered Cu and Ag lamellae with a reduction in average thickness of both Cu ($LT_{Cu} = 46$ nm) and Ag ($LT_{Ag} = 114$ nm) lamellae compared to the sample d_1. For both phases, Cu and Ag, the reduction in thickness is in a similar fashion based on the fact that both have the same slip geometry and uniformity of phase shape and arrangement prior to the deformation [13]. The cold drawing operation from d_1 to d_2 leads to a decrease in grain size and lamellae thickness, although the dislocation density has been increased because of the formation of new dislocations. The reduction in the grain/lamellae size in the sample d_2 creates grain/phase boundary barriers to dislocation motion. Therefore, the motion of dislocations has been delayed which results in increase of the strength of the material d_2.
In general, the texture of the material is influenced by the drawing strain. Therefore, the anisotropy of the material increases with increase in the drawing strain. The deformed texture measured by XRD of sample d_2 is given in terms of pole figures and ODF. Figure 6 and 7 represent the XRD measured textures in the sample d_2. Figure 6 reveals strong texture values for both Cu and Ag phases. Therefore the drawn sample d_2 provides a more pronounced texture than sample d_1. It is observed that the intensity of the texture components increases for both phases with increase in the drawing strain, i.e., from d_1 to d_2.

3.3. EBSD measurements

To investigate the deformed microstructure and orientation information of both phases, we employ EBSD measurements for both samples in transverse direction. Figure 8, 9 show the EBSD results of the drawn samples d_1 and d_2. We use the quantitative EDX information of the copper and silver phases, i.e., the red phase is the Ag rich solid-solution, and the green phase is the Cu rich

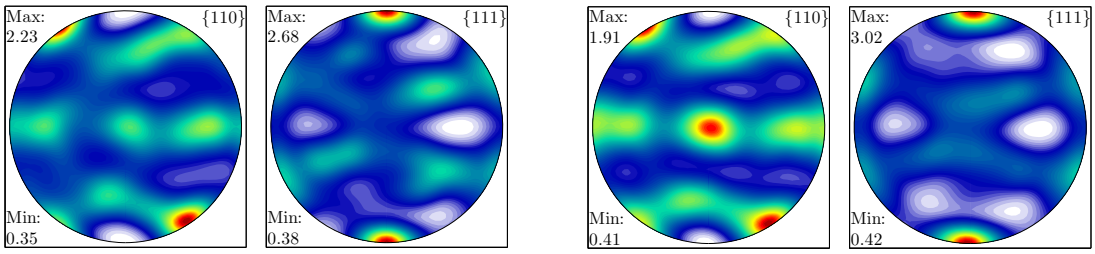

Figure 4: (110), (111) pole figures of the sample d_1. The left figure is for the Ag-phase and the right is for the Cu-phase

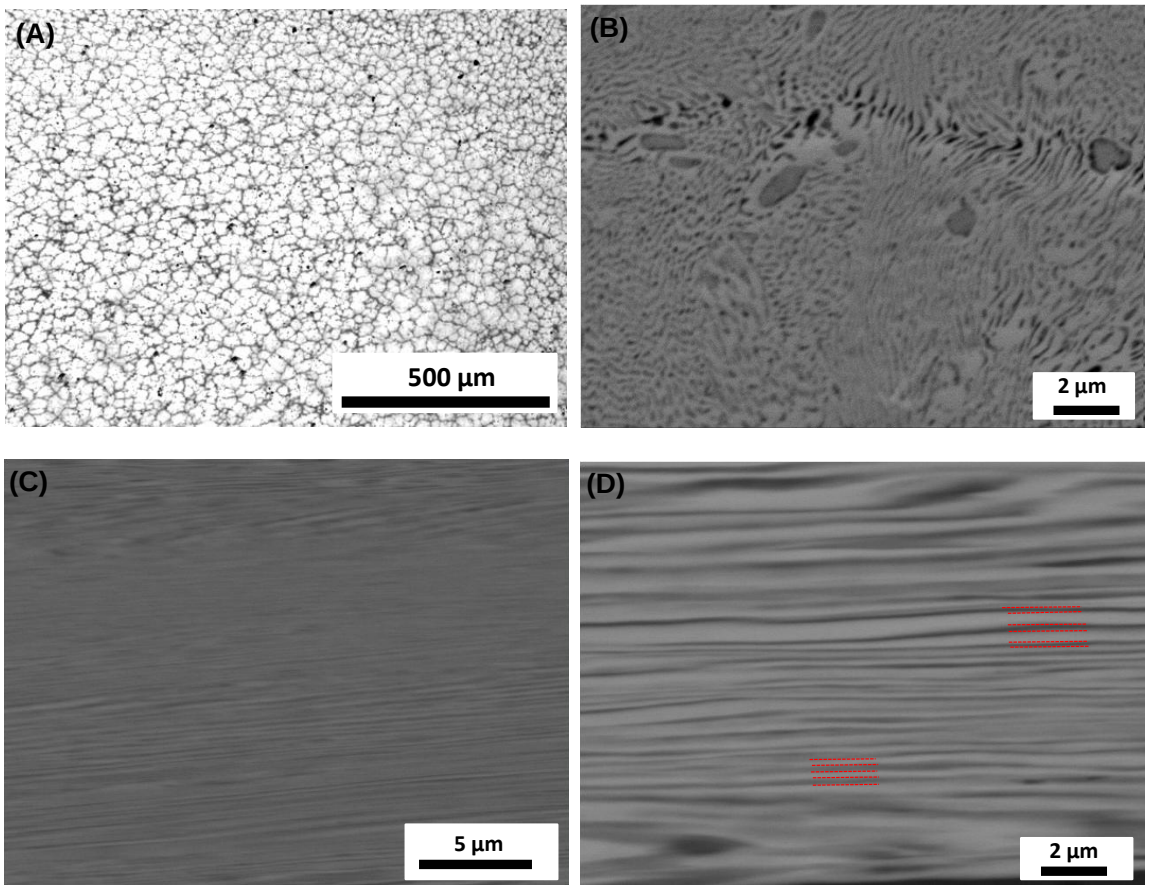

Figure 5: Microstructure of the Cu-Ag drawn sample (d_2): (A), (B) transverse direction T and (C), (D) longitudinal direction L, analyzed by optical and scanning electron microscopy (SEM).

solid-solution, as shown in Figure 8A, 9A. Figures 8B, 8C and Figures 9B, 9C show the orientation maps of the Ag and Cu phases. Both are processed by OIM software. Abundant banded structures in the Ag phase have been observed (see dotted circles in Figure 8B, 9B). In the literature [21], these banded structures are interpreted as twinned regions. In general, the deformation twinning occurs easily in Ag because of its low stacking fault energy [31]. On the other hand, the Cu phase has very few banded structures (see dotted circles in Figure 8C, 9C). This indicates the possibility of the twinned structure inside the Cu and Ag phase. The unexpected formation of twins in the Cu is due to the propagation of twins from the Ag-rich solution into the Cu-rich regions (see also [21] ,[32]).

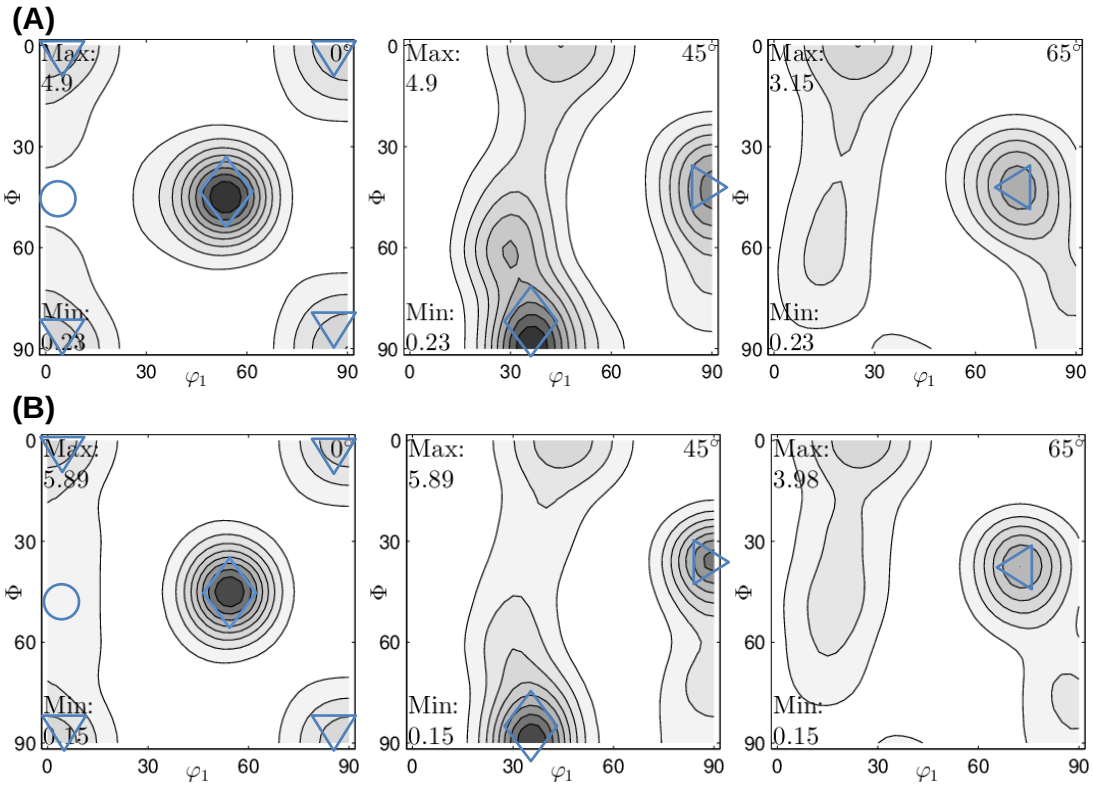

Figure 6: Sample d_2: ODF sections of $\varphi_2 = 0°, 45°, 65°$ in the space of Euler angles with locations of important texture components (∇ - cube orientation ($\{001\}\langle001\rangle$), $\diamondsuit$ - brass orientation ($\{110\}\langle112\rangle$), O - goss orientation ($\{011\}\langle100\rangle$), $\triangleright$ - copper orientation ($\{112\}\langle111\rangle$), $\triangleleft$ - S orientation ($\{123\}\langle634\rangle$)) (A) Ag phase, (B) Cu phase

3.4. Compression tests

The initial texture that develops in materials (d_1, d_2) is not random, hence the stress-strain behavior is anisotropic. The stress-strain curve obtained during compression at a strain rate of $10^{-4}s^{-1}$ for both samples in the two directions (longitudinal and transversal) are shown in Figure 10 and 11. As one can see, the mechanical properties of the drawn sample d_1 and d_2 are direction-dependent (anisotropic). The yield strength value in longitudinal (L) direction is 14% higher than in the transverse direction (T) for the drawn sample d_1. This difference increases to 32% for the drawn sample d_2. The anisotropy in the mechanical properties of the material is due to the crystallographic texture. These results demonstrate that the yield strength increases with increase in the drawing strain, but also depends on the orientation. Figure 10 and 11 show an increase in the strength with increase of wire deformation. The possible reasons for strengthening are the refinement of the microstructure and the evolution of crystallographic texture.

3.5. Texture evolution after compression testing

The compressed samples are once again prepared for the XRD measurements. The texture measurements for the sample d_1 are shown in Figures 12, 13, and for the sample d_2 in Figures 14, 15. The texture evolution after compressive deformation in both phases of the drawn sample d_1 led to typical deformation textures. In the case of the Ag phase, the brass ($\{110\}\langle112\rangle$), goss ($\{011\}\langle100\rangle$), copper ($\{112\}\langle111\rangle$), S ($\{123\}\langle634\rangle$) components are observed, and in the case of Cu phase the cube ($\{001\}\langle001\rangle$), brass ($\{110\}\langle112\rangle$), goss ($\{011\}\langle100\rangle$), copper ($\{112\}\langle111\rangle$), S ($\{123\}\langle634\rangle$) components are observed. The texture development during plastic deformation in both phases of the drawn sample d_1 led to an enhancement of the texture (see Figure 12 and 13 (left)). Both phases have a strong brass component, and the texture becomes stronger compared to the uncompressed material. The Cu and Ag phases have a noticeable difference in the texture

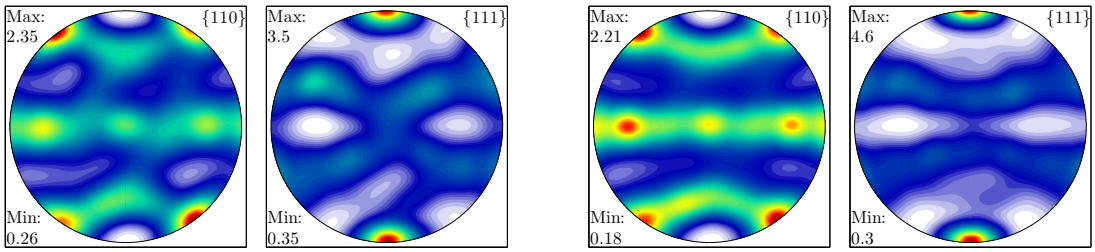

Figure 7: $(110), (111)$ pole figures of the sample d_2. The left figure is for the Ag-phase and the right is for the Cu-phase

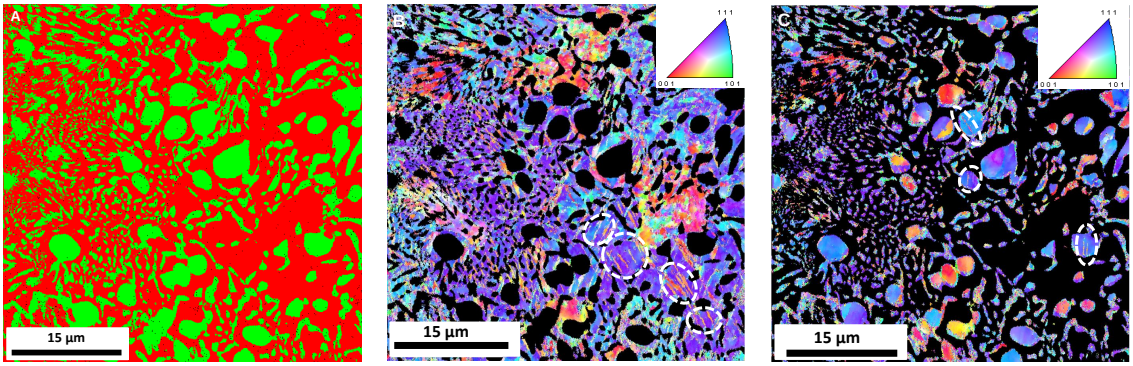

Figure 8: EBSD results of sample d_1: (A) phase color coded map of silver phase (red color) and copper phase (green color), (B) inverse pole figure contrast map of silver phase and (C) inverse pole figure contrast map of copper phase. The black color in (B) and (C) corresponds to removed phase of Cu and Ag. (For interpretation of the references to color in this figure legend, the reader is referred to the web version of this article.)

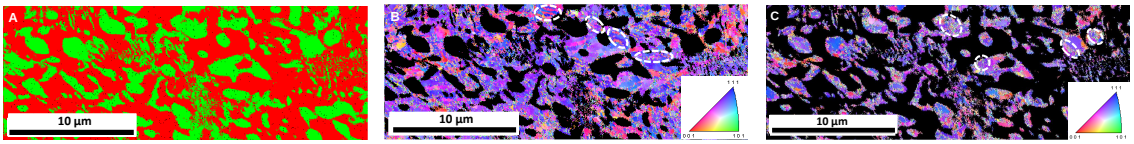

Figure 9: EBSD results of sample d_2: (A) phase color coded map of silver phase (red color) and copper phase (green color), (B) inverse pole figure contrast map of silver phase and (C) inverse pole figure contrast map of copper phase. The black color in (B) and (C) corresponds to removed phase of Cu and Ag.

intensities. One can see in Figure 12 that the $\varphi_2(= 0°, 45°)$ sections develop a strong brass component ($\{110\}\langle 112\rangle$). The texture intensity is high for the Ag phase, and it can be clearly seen that the Ag brass texture component is the dominant component being responsible for the deformation of the material with an Ag rich phase and the Ag lamellae. Figure 14 reveals that the increase in the texture intensity is not observed in both phases since the minimum intensity is recorded in the X-ray diffraction for both the phases. Possible reasons for this decline in intensity could be explained by dispersion of diffraction peaks in both the Cu and Ag phases observed at high strains in the eutectic rolled and drawn materials, and hence corresponds to a decline in X-ray counts during the measurement (see also [13, 24]).

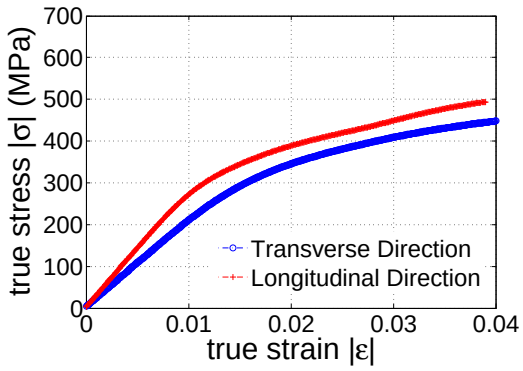

Figure 10: Comparion of true stress versus true strain curves of sample $d_1 = 12.42$ mm.

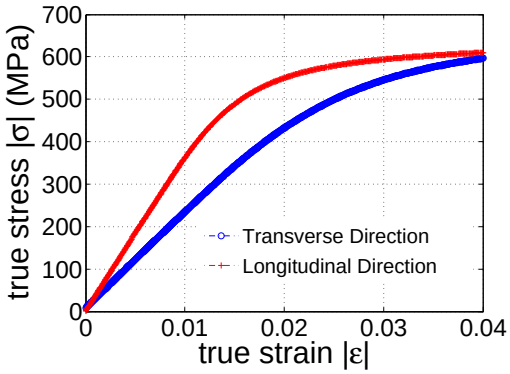

Figure 11: Comparsion of true stress versus true strain curves of sample $d_2 = 6.73$ mm.

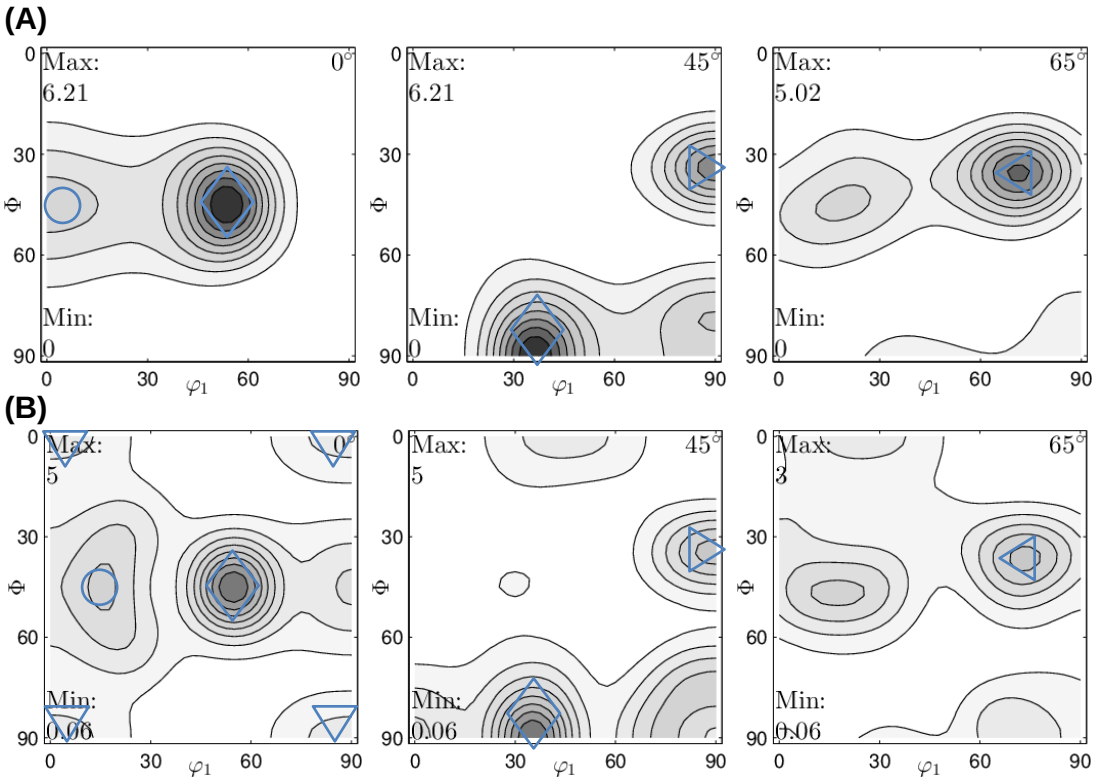

Figure 12: ODF sections of $\varphi_2 = 0°, 45°, 65°$ in the space of Euler angles showing the measured texture with locations of important texture components (∇ - cube orientation $(\{001\}\langle001\rangle)$, $\diamondsuit$ - brass orientation $(\{110\}\langle112\rangle)$, O - goss orientation $(\{011\}\langle100\rangle)$, $\triangleright$ - copper orientation $(\{112\}\langle111\rangle)$, $\triangleleft$ - S orientation $(\{123\}\langle634\rangle)$) of the compressed sample d_1 with a deformation of 4 %. (A) the Ag phase and (B) the Cu phase.

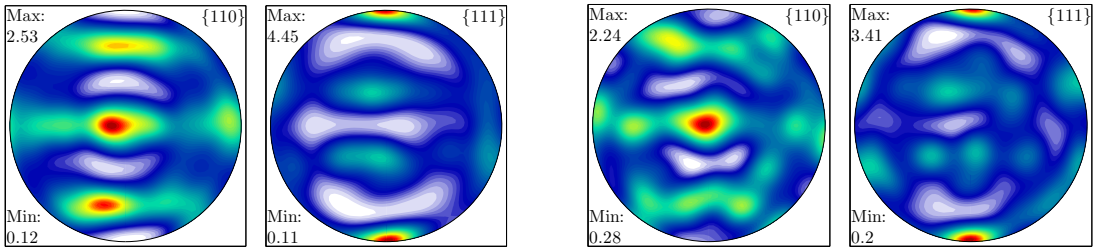

Figure 13: $(110), (111)$ pole figures of the sample d_1 after compression testing with a deformation of 4 %. The left figure is for the Ag-phase and the right is for the Cu-phase.

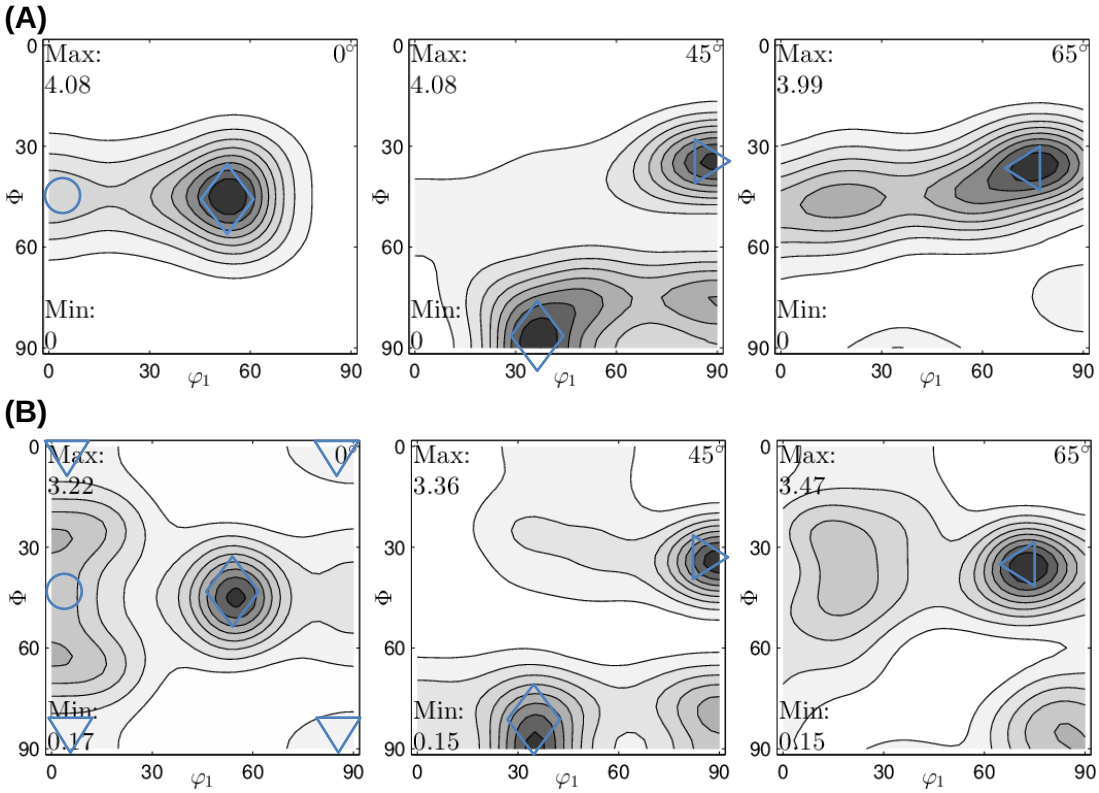

Figure 14: ODF sections of $\varphi_2 = 0°, 45°, 65°$ in the space of Euler angles showing the measured texture with locations of important texture components (∇ - cube orientation $(\{001\}\langle 001\rangle)$, $\diamondsuit$ - brass orientation $(\{110\}\langle 112\rangle)$, O - goss orientation $(\{011\}\langle 100\rangle)$, $\triangleright$ - copper orientation $(\{112\}\langle 111\rangle)$, $\triangleleft$ - S orientation $(\{123\}\langle 634\rangle)$) of the compressed sample d_2 with a deformation of 5 %. (A) Ag phase and (B) the Cu phase.

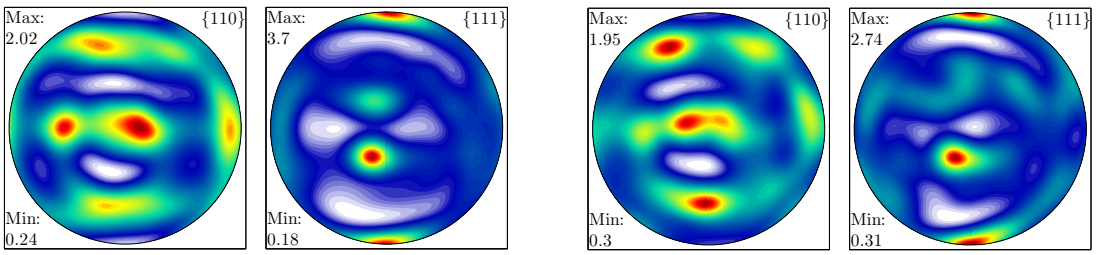

Figure 15: $(110), (111)$ pole figures of the sample d_2 after compression testing with a deformation of 5 %. The left figure is for the Ag-phase, and the right is for the Cu-phase.

4. Conclusions

In conclusion, a comparison of two different cold drawn Cu-Ag composites exposes a correlation on the microstrcture, initial texture, compressive deformation behavior, and the final texture. For both samples, the findings of a higher yield strength in the longitudinal direction reveals the presence of anisotropy. The anisotropic characteristics are also manifested in the true stress-strain curves for both drawn samples. It has been noted that banded structures and crystallographic texture introduce anisotropic mechanical behavior to the composites. These banded structures have been visualized from the EBSD measurements. Abundant banded structures are observed in the Ag phase, whereas very few banded structures are observed in the Cu phase. Both phases of the drawn samples initially have the same alloy type texture as shown in ODF plots. The texture intensity increases for both phases as the drawing strain increases i.e., from sample d_1 to d_2. Texture measurements after compression tests of both samples reveal that the texture becomes more pronounced.
The increase in the yield strength from the sample d_1 to d_2 is observed due to the development of fine microstructure, the evolution of texture, and the refinement of banded structures. With increase in the drawing strain i.e, d_1 to d_2, the banded regions are more refined and also influence the strength of the conductor materials. Therefore for the design of new and improved Cu-Ag composite materials for a high strength conductors, one must control the banded structures present in the starting material.

5. Acknowledgements

We thank Dr. Jens Freudenberger (IFW Dresden) for providing the samples for our investigations. We sincerely thank Prof. Thorsten Halle (University of Magdeburg) for proposing EBSD measurements and the contact with Dr. D. Dietrich (TU Chemnitz). We thank A. Hilbig and H.Voß for assistance in XRD measurements, M. Ecke and H. Heyse for their assistance in carrying out the SEM. Financial assistance from GRK1554 is gratefully acknowledged.

References

[1] G. Gottstein F. Heringhaus, H. J. Schneider-Muntau. Analytical modeling of the electrical conductivity of metal matrix composites: application to Ag-Cu and Cu-Nb. Materials Science and Engineering A, 347:9–20, 2003.

[2] W. Grünberger, M. Heilmaier, and L. Schultz. High-strength pearlitic steel-copper composite wires for conductors in pulsed high-field magnets. Materials Science and Engineering A, 303: 127–133, 2001.

[3] W. Grünberger, M. Heilmaier, and L. Schultz. High-strength, high-nitrogen stainless steel-copper composite wires for conductors in pulsed high-field magnets. Materials Letters, 52: 154–158, 2002.

[4] C A Davy, K Han, P N Kalu, and S T Bole. Examinations of Cu-Ag composite conductors in sheet forms. IEEE Transactions on Applied Superconductivity, 18:560–563, 2008.

[5] Y. Sakai, T. Asano, K. Inoue, H. Wada, and H. Maeda. Development of high strength, high conductivity Cu-Ag alloys for high field pulsed magnet use. Applied Physics Letters, 59: 2965–2967, 1991.

[6] Y. Sakai, K. Inoue, and H. Maeda. New high-strength, high-conductivity Cu-Ag alloy sheets. Acta metall. mater., 43:1517–1522, 1995.

[7] Y. Sakai and H. J. Schneider-Muntau. Ultra-high strength, high conductivity Cu-Ag alloy wires. Acta materiala, 45:1017–1023, 1997.

[8] T. Asano, Y. Sakai, K. Inoue, M. Oshikiri, and H. Maeda. High-field pulsed magnet wound of Cu-Ag alloy wire. Japanese Journal of Applied Physics, 32:L1027–L1029, 1993.

[9] W Grünberger, M Heilmaier, and L Schultz. Development of high-strength and high-conductivity conductor materials for pulsed high-field magnets at Dresden. Physica B, 45: 643–647, 2001.

[10] Srihari Dodla, A. Bertram, and M. Krüger. Finite element simulation of lamellar copper-silver composites. Computational Materials Science, 101:29–38, 2015.

[11] A. Gaganov, J. Freudenberger, W. Grünberger, and L. Schultz. Microstructural evolution and its effect on the mechanical properties of Cu-Ag microcomposites. Z. Metallkd., 95:425–432, 2004.

[12] W. Grünberger, M. Heilmaier, and L. Schultz. Microstructure and mechanical properties of Cu-Ag microcomposites for conductor wires in pulsed high-field magnets. Z. Metallkd., 93: 58–65, 2002.

[13] F. Heringhaus. Quantitative Analysis of the Influence of th Microstructure on Strength, Resistivity, and Magnetoresistance of Eutectic Silver-Copper. Shaker Verlag, Berlin, 1998.

[14] G Frommeyer and G Wassermann. Microstructure and anomalous mechanical properties of in situ-produced silver-copper composite wires. Acta Metallurgica, 23:1353–1360, 1975.

[15] K Han, J D Embury, J R Sims, L J Campbell, H J Schneider Muntau, V I Pantsyrnyi, A Shikov, A Nikulin, and A Vorobieva. The fabrication, properties and microstructure of Cu-Ag and Cu-Nb composite conductors. Materials Science and Engineering A, 267:99–114, 1999.

[16] S. Suwas, L. S. Toth, J. J. Fundenberger, A. Eberhardt, and W. Skrotzki. Evolution of crystallographic texture during equal channel angular extrusion of silver. Scripta Materialia, 49:1203–1208, 2003.

[17] I. J. Beyerlein, L. S. Toth, C. N. Tome, and S. Suwas. Role of twinning on texture evolution of silver during equal channel angular extrusion. Philosophical Magazine, 87:885–906, 2007.

[18] J. S. Carpenter, S. C. Vogel, J. E. LeDonne, D. L. Hammon, I. J. Beyerlein, and N. A. Mara. Bulk texture evolution of Cu-Nb nanolamellar composites during accumulative roll bonding. Acta Materialia, 60:1576–1586, 2012.

[19] I. J. Beyerlein, N. A. Mara, and J. S. Carpenter. Interface-driven microstructure development and ultra high strength of bulk nanostructured Cu-Nb multilayers fabricated by severe plastic deformation. J. Mater. Res., 28:1799–1812, 2013.

[20] A. Kauffmann, J. Freudenberger, H. Klauß, W. Schillinger, V. Subramanya Sarma, and L. Schultz. Efficiency of the refinement by deformation twinning in wire drawn single phase copper alloys. Materials Science & Engineering A, 624:71–78, 2015.

[21] Irene J. Beyerlein, Nathan A. Mara, Dhriti Bhattacharyya, David J. Alexander, and Carl T. Necker. Texture evolution via combined slip and deformation twinning in rolled silver - copper cast eutectic nanocomposite. International Journal of Plasticity, 27:121–146, 2011.

[22] E. Dieter, G. Mechanical metallurgy (3rd ed.). Boston: McGraw Hill, 1986. ISBN 0070168938.

[23] U F Kocks, C N Tome, and H R Wenk. Texture and Anisotropy: Preferred Orientations in Polycrystals and thier Effect on Materials Properties. Cambridge University Press, 1998. ISBN 978-0521794206.

[24] Charney. A. Davy. A study of nanostructured Copper-Silver composites. The Florida State University Press, 2010. ISBN 9781124680408.

[25] R. Hielscher and H. Schaeben. A novel pole figure inversion method: specification of the *MTEX* algorithm. Journal of Applied Crystallography, 41(6):1024–1037, Dec 2008. doi: 10.1107/S0021889808030112. URL http://dx.doi.org/10.1107/S0021889808030112.

[26] Florian Bachmann, Ralf Hielscher, Peter E. Jupp, Wolfgang Pantleon, Helmut Schaeben, and Elias Wegert. Inferential statistics of electron backscatter diffraction data from within individual crystalline grains. Journal of Applied Crystallography, 43(6):1338–1355, Dec 2010. doi: 10.1107/S002188981003027X. URL http://dx.doi.org/10.1107/S002188981003027X.

[27] Ralf Hielscher, Helmut Schaeben, and Heinrich Siemes. Orientation distribution within a single hematite crystal. Mathematical Geosciences, 42:359–375, 2010. ISSN 1874-8961. doi: 10.1007/s11004-010-9271-z. URL http://dx.doi.org/10.1007/s11004-010-9271-z.

[28] F. Bachmann, R. Hielscher, and H. Schaeben. Texture analysis with MTEX–free and open source software toolbox. Solid State Phenomena, 160:63–68, 2010. doi: 10.4028/www.scientific.net/SSP.160.63. URL http://dx.doi.org/10.4028/www.scientific.net/SSP.160.63.

[29] S. Mahesh, C. N. Tome, R. J. McCabe, G. C. Kaschner, I. J. Beyerlein, and A. Misra. A sub-structure based hardening model for copper under loading path changes. Metall. Mater. Trans. A, 35A:3763–3774, 2004.

[30] H. Hu and R.S. Cline. Temperature dependence of rolling textures in high-purity silver. Journal of Applied Physics, 32:760–763, 1961.

[31] E. B. Tadmor and N. Bernstein. A first-principles measure for the twinnability of FCC metals. Journal of the Mechanics and Physics of Solids, 52:2507–2519, 2004.

[32] Y. Z. Tian and Z.F. Zhang. Bulk eutectic Cu-Ag alloys with abundant twin boundaries. Scripta Materialia, 66:65–68, 2012.